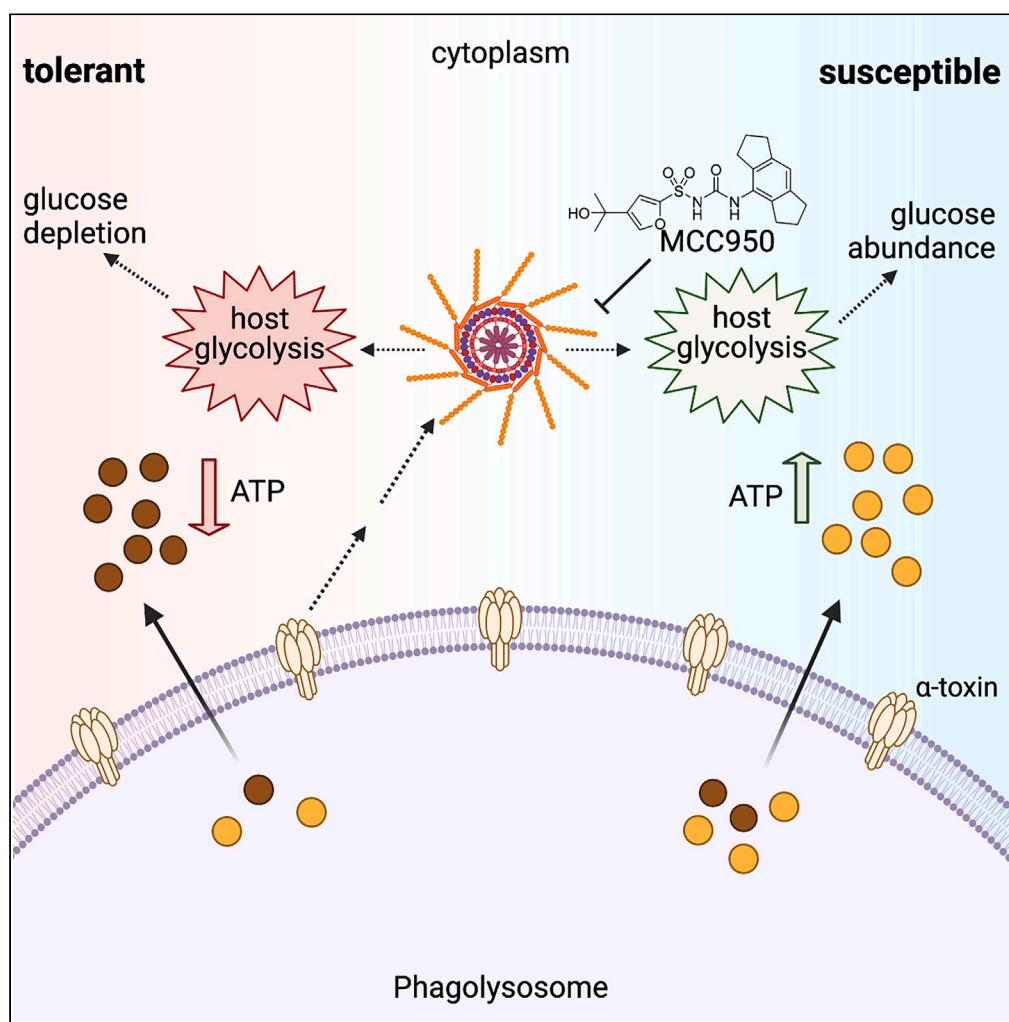


Article

Inflammasome-mediated glucose limitation induces antibiotic tolerance in *Staphylococcus aureus*

Jenna E. Beam,
Nikki J. Wagner,
Kuan-Yi Lu, Joshua
B. Parsons, Vance
G. Fowler, Jr.,
Sarah E. Rowe,
Brian P. Conlon

brian_conlon@med.unc.edu

Highlights

Staphylococcus aureus activates the NLRP3 inflammasome in macrophages

NLRP3 activation leads to depletion of glucose in the macrophage cytoplasm

Reduced glucose availability induces antibiotic tolerance in *S. aureus*

Restoration of cytoplasmic glucose improves antibiotic efficacy

Beam et al., iScience 26, 107942
October 20, 2023 © 2023 The Author(s).
<https://doi.org/10.1016/j.isci.2023.107942>

Article

Inflammasome-mediated glucose limitation induces antibiotic tolerance in *Staphylococcus aureus*

Jenna E. Beam,^{1,4} Nikki J. Wagner,^{1,4} Kuan-Yi Lu,¹ Joshua B. Parsons,^{1,3} Vance G. Fowler, Jr.,³ Sarah E. Rowe,¹ and Brian P. Conlon^{1,2,5,*}

SUMMARY

***Staphylococcus aureus* is a leading human pathogen that frequently causes relapsing infections. The failure of antibiotics to eradicate infection contributes to infection relapse. Host-pathogen interactions have a substantial impact on antibiotic susceptibility and the formation of antibiotic tolerant cells. In this study, we interrogate how a major *S. aureus* virulence factor, α -toxin, interacts with macrophages to alter the microenvironment of the pathogen, thereby influencing its susceptibility to antibiotics. We find α -toxin-mediated activation of the NLRP3 inflammasome induces antibiotic tolerance. Induction of tolerance is driven by increased glycolysis in the host cells, resulting in glucose limitation and ATP depletion in *S. aureus*. Additionally, inhibition of NLRP3 activation improves antibiotic efficacy *in vitro* and *in vivo*, suggesting that this strategy has potential as a host-directed therapeutic to improve outcomes. Our findings identify interactions between *S. aureus* and the host that result in metabolic crosstalk that can determine the outcome of antimicrobial therapy.**

INTRODUCTION

Staphylococcus aureus (*S. aureus*) is the causative agent of multiple invasive infections, with high rates of morbidity and mortality.^{1,2} In 2017, *S. aureus* sepsis contributed to over 20,000 patient deaths in the US alone.² Despite antibiotic therapy availability, treatment failure is common and often attributed to the formation of antibiotic tolerant cells.^{2–4}

Antibiotic tolerance is generally defined as an increased capacity of a bacterial population to survive for prolonged periods in the presence of bactericidal antibiotics. Antibiotic tolerance can occur as bacteria enter a basal metabolic state, characterized by low levels of ATP.^{5–8} We have previously shown that reactive oxygen/nitrogen species (ROS/RNS) induce antibiotic tolerance via collapse of the tricarboxylic acid (TCA) cycle and ATP depletion within hours after macrophage infection^{5,6} and similar induction of antibiotic tolerance by macrophages has been characterized in *Mycobacterium tuberculosis* and *Salmonella*.^{9,10} In broth culture, glucose supplementation has been shown to resuscitate antibiotic tolerant cells by increasing their ATP levels,⁷ and the addition of exogenous glucose increased antibiotic susceptibility, even in the absence of a functional TCA cycle.⁵ *S. aureus* virulence and proliferation *in vivo* is highly dependent on glucose and the presence of four glucose transporters demonstrate the importance of glucose acquisition to this pathogen.¹¹

Due to the limitations of currently approved antibiotics and a striking lack of new antibiotics in the pipeline, identifying and developing anti-virulence and/or host-directed therapeutics for the treatment of bacterial infections is becoming increasingly attractive.^{6,12–17} We hypothesized that conditions altering accessible glucose in the immediate proximity of *S. aureus* could increase antibiotic efficiency.

One of the major classes of virulence factors in *S. aureus* are the pore-forming toxins, including α -toxin and leukocidins, such as γ -hemolysin, PVL, LukE, and LukAB. These toxins contribute to host cell death, initiate host cell signaling cascades, such as inflammasome activation, and mediate pathogen dissemination by facilitating escape from the host cell.^{13,17–21} Antibody-mediated neutralization of α -toxin has been shown to improve infection outcome in animal models of pneumonia, bacteremia, and skin and soft tissue infections^{13,16,22–24} and the presence of anti- α -toxin antibodies correlates with better clinical outcomes in sepsis and skin infections.²⁵ While neutralization of α -toxin can contribute to improved infection outcomes, the role of α -toxin in antibiotic efficacy has not been determined.

Upon encountering immune cells, *S. aureus* virulence factors, such as α -toxin and leukocidins, initiate an innate immune response that includes activation of Toll-like receptors (TLRs), NOD-like receptors (NLRs) and the NLR pyrin domain-containing protein 3 (NLRP3) inflammasome.^{20,21} While this host response is critical for controlling *S. aureus* infection,^{26,27} α -toxin-mediated activation of the NLRP3 inflammasome also contributes to *S. aureus* pathogenicity.^{13,20,28,29} Additionally, activation of NLRP3 has been shown to modulate host cell

¹Department of Microbiology and Immunology, University of North Carolina at Chapel Hill, Chapel Hill, NC 27599, USA

²Marsico Lung Institute, University of North Carolina at Chapel Hill, Chapel Hill, NC 27599, USA

³Division of Infectious Diseases, Duke University School of Medicine, Durham, NC, USA

⁴These authors contributed equally

⁵Lead contact

*Correspondence: brian_conlon@med.unc.edu

<https://doi.org/10.1016/j.isci.2023.107942>



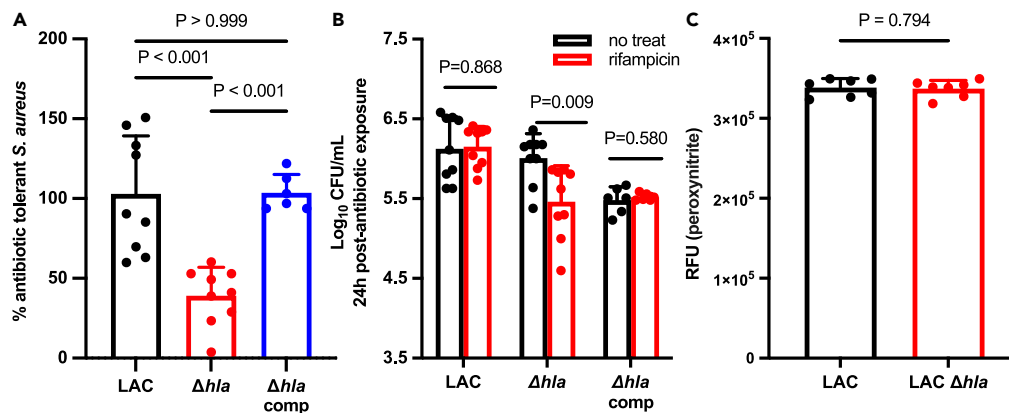


Figure 1. Loss of α -toxin increases antibiotic susceptibility in macrophages

(A and B) BMDMs were infected at MOI 10 for 45 min, followed by treatment with 10 $\mu\text{g}/\text{ml}$ rifampicin for 24 h. % survival (A) was extrapolated from CFU/ml (B). (C) Peroxynitrite levels in BMDMs infected with LAC or LAC Δhla . Peroxynitrite levels were measured by FI-B fluorescence. See also Figure S1. Statistical significance was determined by one-way ANOVA with Sidak's multiple comparison (A) or unpaired t-test (two-tailed) (B and C). All experiments were performed in biological triplicate at least twice on two separate days ($n \geq 6$). Bars represent the mean \pm standard deviation. See also Figure S1 and Table S1.

glycolysis.^{30–33} While the interaction between α -toxin and NLRP3 activation is well documented, the role of this interaction in antibiotic treatment outcome has not been determined.

In the current study, we aimed to determine if α -toxin-mediated activation of NLRP3 contributes to the formation of antibiotic tolerant *S. aureus* and if targeting activation of the NLRP3 signaling pathway is a potential host-directed therapeutic strategy that synergizes with antibiotic treatment.

RESULTS

Loss of α -toxin decreases antibiotic tolerance

To determine the role of α -toxin in antibiotic tolerance, bone marrow-derived macrophages (BMDMs) from C57BL/6 mice and THP-1 human monocyte-derived macrophages (hMDMs) were infected with *S. aureus* wildtype (WT) strain LAC or an α -toxin deletion mutant, LAC Δhla , followed by treatment with rifampicin (Figures 1A and 1B) or moxifloxacin (Figures S1A and S1B). Both rifampicin and moxifloxacin were chosen as these drugs are bactericidal and readily penetrate macrophages by passive diffusion.^{34,35} At 24 h post-infection (hpi), macrophages were lysed and colony forming units (CFU) were enumerated. Treatment with both antibiotics resulted in increased killing of intracellular LAC Δhla compared to intracellular WT LAC, suggesting that α -toxin mediates antibiotic tolerance (Figures 1A, 1B, S1A, and S1B). To determine if this phenotype was strain specific, another WT strain, HG003, was used to infect BMDMs as described above (Figures S1C and S1D). Infected cells were treated with a more clinically relevant antibiotic combination of vancomycin and rifampicin.³⁶ As in the LAC background, the HG003 Δhla mutant was less tolerant to antibiotic treatment. The same decreased antibiotic tolerance of the Δhla mutant was also observed in THP-1 hMDMs (Figures S1E and S1F). The minimum inhibitory concentration (MIC) of rifampicin, moxifloxacin, and vancomycin were unchanged between WT LAC and LAC Δhla mutant strain (Table S1), demonstrating that the phenotype we observed was not due to a change in antibiotic resistance. These data indicate that α -toxin mediates antibiotic tolerance in macrophages.

We have previously shown that, in the phagolysosome, high levels of ROS, specifically peroxynitrite, induce an antibiotic tolerant state in *S. aureus* via collapse of central metabolism and reduced levels of ATP.^{5,6} Given the high immunogenicity of α -toxin, we reasoned that perhaps macrophages that have phagocytosed *S. aureus* without α -toxin would be less activated than those engulfing WT *S. aureus*, leading to lower levels of ROS and thus fewer antibiotic tolerant bacteria.³⁷ To measure ROS, BMDMs were infected with either WT LAC or LAC Δhla for 1 h, followed by addition of the ROS-sensitive luminescent probe L-012 or staining with fluorescein-boronate (FI-B; measures peroxynitrite).³⁸ However, no differences in ROS levels were observed between WT or Δhla infected macrophages (Figures 1C and S1G), indicating that α -toxin mediates antibiotic tolerance in macrophages independently of ROS.

Inhibition of NLRP3 decreases antibiotic tolerance

Multiple studies have shown that α -toxin is a potent activator of the NLRP3 inflammasome.^{13,20,39,40} Canonical NLRP3 activation is a two-signal process, where signal 1 is a priming step, typically TLR signaling downstream of pattern-recognition receptor (PAMP) sensing. This leads to activation of NF- κ B and increased expression of NLRP3 monomers, pro-IL-1 β and pro-IL-18. Upon receiving signal 2, NLRP3 monomers activate and oligomerize.^{41,42} Signal 2 can be initiated by a variety of stimuli, including changes in calcium ion flux, mitochondrial damage, or, in the case of α -toxin, formation of membrane pores that lead to potassium ion efflux.^{13,20} To examine if NLRP3 activation contributes to the induction of antibiotic tolerance, we first measured caspase-1 activation and LDH secretion as proxies for NLRP3 activation following infection with LAC or LAC Δhla . BMDMs infected with WT LAC exhibited increased caspase-1 activation (Figure 2A) and LDH release (Figure 2B)

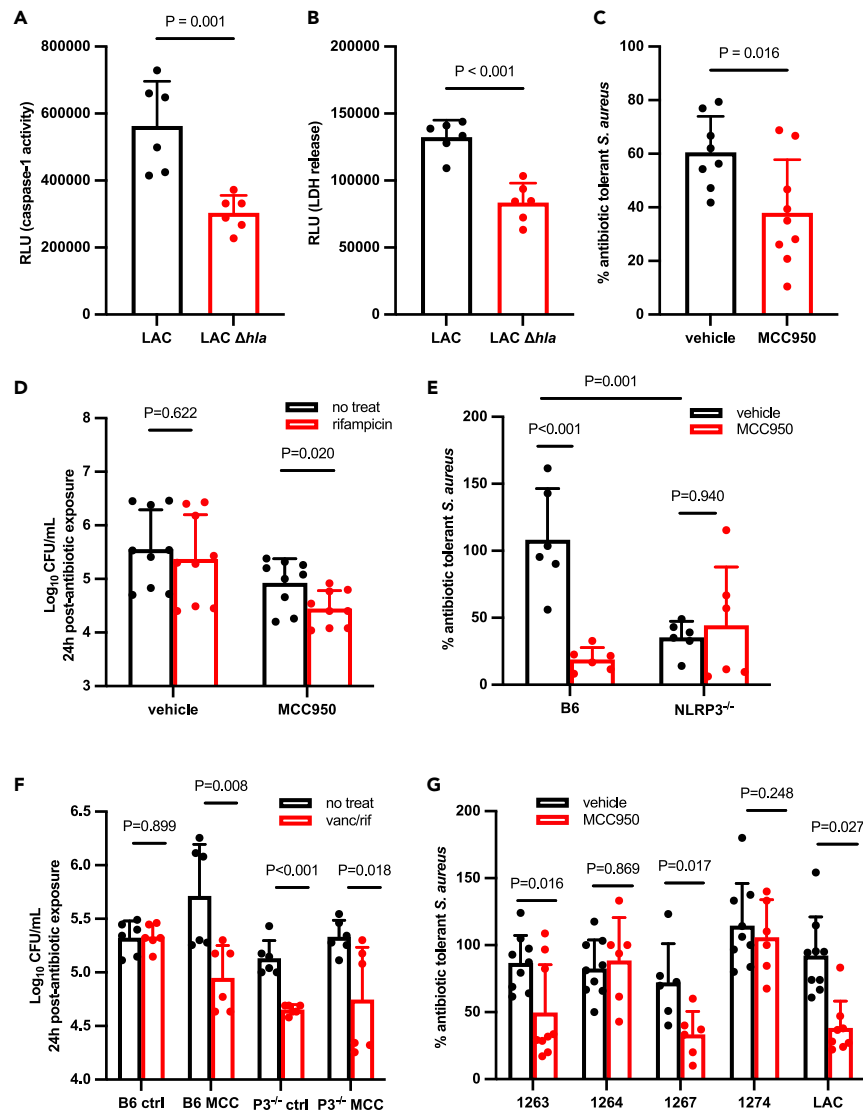


Figure 2. NLRP3 inhibition increases antibiotic susceptibility of *S. aureus*

(A and B) WT BMDMs were infected with LAC or LAC Δhla for 24 h followed by measurement of caspase-1 activity by luminescence (A) or quantification of LDH levels (B).

(C and D) BMDMs were exposed to 10 ng/ml lipopolysaccharide (LPS) for 4 h, followed by replacement with serum-free media containing 10 μ M MCC950 for 30 min prior to infection with WT LAC and treatment with 10 μ g/ml rifampicin for 24 h. % survival (C) was extrapolated from CFU/ml at 24hpi (D).

(E and F) WT (B6) or NLRP3 deficient ($P3^{-/-}$) BMDMs were treated and infected with WT LAC as above before being exposed to 50 μ g/ml vancomycin and 10 μ g/ml rifampicin. % survival (E) was extrapolated from CFU/ml (F).

(G) WT BMDMs were treated and infected as above using *S. aureus* isolated from bacteremia patients. % survival after 24 h with 50 μ g/ml vancomycin and 10 μ g/ml rifampicin was extrapolated from CFU/ml (Figure S3A). See also Figure S2 and Figure S3. Statistical significance was determined by two-tailed unpaired t-test (A, B, C, D, F, and G) or one-way ANOVA with Sidak's multiple comparison (E). All experiments were performed in biological triplicate at least twice on two separate days ($n \geq 6$). Bars represent the mean \pm standard deviation. See also Figures S2 and S3.

compared to LAC Δhla infected BMDMs. Next, we treated BMDMs with NLRP3 signaling inhibitors, MCC950 or oridonin, prior to infection with LAC and antibiotic treatment.^{43,44} Inhibition of NLRP3 decreased antibiotic tolerance in *S. aureus* (Figures 2C, 2D, S2A, and S2B). In BMDMs infected with Δhla , MCC950 had no significant effect, although there was reduced tolerance, likely due to activation of NLRP3 by other bacterial factors²¹ (Figures S2C and S2D). To verify that treatment with NLRP3 inhibitors did not damage the macrophages, thereby altering the recovered CFU, CellTiter-Blue was used to measure macrophage viability. No difference was seen between WT LAC-infected macrophages treated with MCC950 or vehicle (Figure S2E). To further confirm that NLRP3 contributes to tolerance, BMDMs were derived from mice deficient in NLRP3 (B6.129S6-Nlrp3^{tm1Bhk}).⁴⁵ We reasoned that if NLRP3 activation is sufficient to induce tolerance, *S. aureus* phagocytosed by NLRP3-deficient macrophages will not exhibit antibiotic tolerance. WT LAC was less antibiotic tolerant in NLRP3-deficient

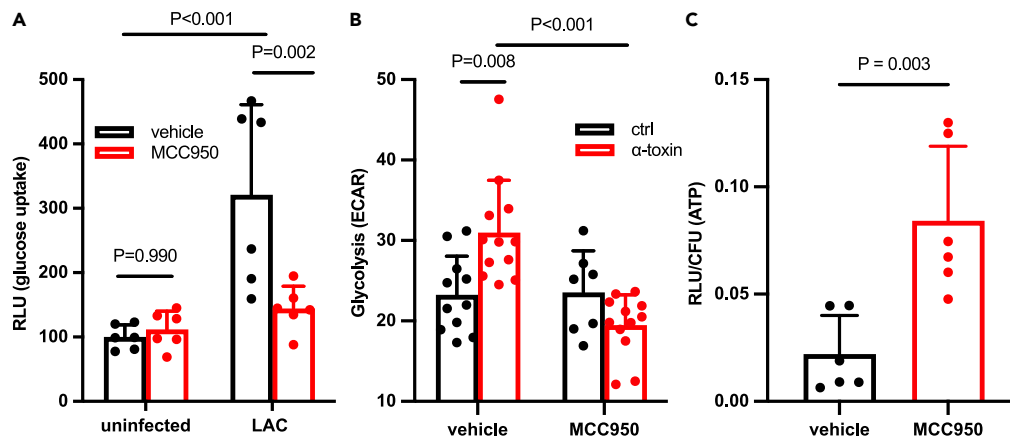


Figure 3. NLRP3 activation alters macrophage glycolysis causing a decrease of ATP in *S. aureus*

(A) Glucose uptake into BMDMs was measured at 24 hpi using the Glucose Uptake-Glo assay kit (Promega). BMDMs were primed for 4h with 10 ng/ml LPS, followed by treatment with 10 μ M MCC950 or vehicle (DMSO) for 45 min and infection at MOI 10 with WT LAC. Data were normalized to RLU from uninfected samples.

(B) Seahorse XF Glycolysis Stress Assay was used to measure glycolysis from BMDMs untreated or treated with 100 μ M MCC950 followed by stimulation with 50 ng/ml alpha toxin.

(C) ATP levels in *S. aureus* as measured by luminescence. BMDMs treated with and without MCC950 prior to infection at MOI 10 with LAC*luxABDCE*. Luminescence was measured and normalized to CFU. See also Figure S4. Statistical significance was determined using one-way ANOVA with Sidak's multiple comparison (A, B) or using an unpaired t-test (two-tailed) (C). All experiments were performed in biological triplicate at least twice on two separate days ($n \geq 6$). Bars represent the mean +standard deviation. See also Figure S4.

macrophages compared to BMDMs from WT C57BL/6 mice (Figures 2E and 2F). We then tested *S. aureus* isolates from bacteremia patients to determine if NLRP3-mediated tolerance has clinical relevance. All isolates expressed α -toxin and had a similar MIC to rifampicin (Figure S3B; ⁶). When treated with MCC950, two of the four strains we tested had decreased antibiotic tolerance, suggesting that NLRP3 activation contributes to antibiotic tolerance under these experimental conditions (Figures 2G and S3A). The reasons for a lack of inflammasome-induced tolerance in two of the strains remains unclear, although possible explanations include altered phagosomal escape and intracellular localization, differential induction of respiratory burst and associated TCA cycle collapse, variation in intracellular α -toxin expression levels, and/or variable production of other pore-forming toxins, to name a few.^{17,46–49} Regardless, these data show that NLRP3 activation can induce antibiotic tolerance in *S. aureus* and inhibition of NLRP3 improves antibiotic efficacy in macrophages.

α -toxin-mediated NLRP3 activation increases host cell glycolysis resulting in lower bacterial ATP

Next, we aimed to determine how NLRP3 activation contributes to the induction of antibiotic tolerance. TLR stimulation by bacterial PAMPs and NLRP3 activation have been shown to increase host cell glycolytic activity.^{30–33} Additionally, *S. aureus*-infected non-professional phagocytes have decreased levels of intracellular glucose.⁵⁰ We hypothesized that α -toxin-mediated NLRP3 activation leads to increased host glycolysis, resulting in depletion of host cytoplasmic glucose, leading to antibiotic tolerance in *S. aureus* via nutrient deprivation. Changes in host cell cytoplasmic glucose will more likely influence *S. aureus* if the bacteria have escaped the phagolysosome and entered the cytoplasm.⁵¹ To verify *S. aureus* is in the cytoplasm at the time we see antibiotic tolerance, we performed confocal microscopy on J774A.1 macrophages infected with WT LAC expressing GFP. At 24 hpi, WT LAC was predominantly visible in the macrophage cytoplasm (Figure S4). These data indicate that 24 hpi *S. aureus* is cytoplasmic in J774A.1 cells and therefore could be impacted by host cell cytoplasmic glucose availability.

To investigate changes in cytoplasmic glucose, we measured glucose uptake in untreated and MCC950-treated BMDMs following 24h infection with WT LAC using the Glucose Uptake-Glo Assay. After 24h, BMDMs were treated with 2-deoxyglucose (2DG), a glucose analog that is phosphorylated to 2-deoxyglucose-6-phosphate (2DG6P) but cannot be further metabolized by the host cell. Addition of glucose-6-phosphate dehydrogenase leads to reduction of NADP⁺ to NADPH, which converts pro-luciferin to luciferin. Relative light units (RLU) are therefore proportional to 2DG uptake into the host cells, which is indicative of host cell glucose uptake. BMDMs infected with WT *S. aureus* exhibited increased glucose uptake, which was ameliorated by MCC950 treatment (Figure 3A). To directly assess changes in host glycolysis, we used the Seahorse XF Glycolytic Stress assay on BMDMs exposed to α -toxin with and without MCC950 treatment. This assay measures glycolysis in live cells by quantifying proton efflux specific to glycolysis. As shown in Figure 3B, α -toxin treatment caused increased glycolysis in host cells, which was reduced when the cells were treated with MCC950 prior to α -toxin exposure. These data indicate that inhibition of NLRP3 decreases host cell glycolysis, which correlates with reduced antibiotic tolerant cells. Next, we assessed the metabolic state of the bacteria in untreated or MCC950-treated BMDMs. We reasoned that increased availability of cytoplasmic glucose in MCC950-treated macrophages would result in high levels of ATP in *S. aureus*. To test this, we measured ATP in LAC that was transduced with a chromosomal *luxABDCE* cassette. The bioluminescent reaction is ATP-dependent and has been used as a proxy for bacterial ATP levels.⁵² BMDMs were

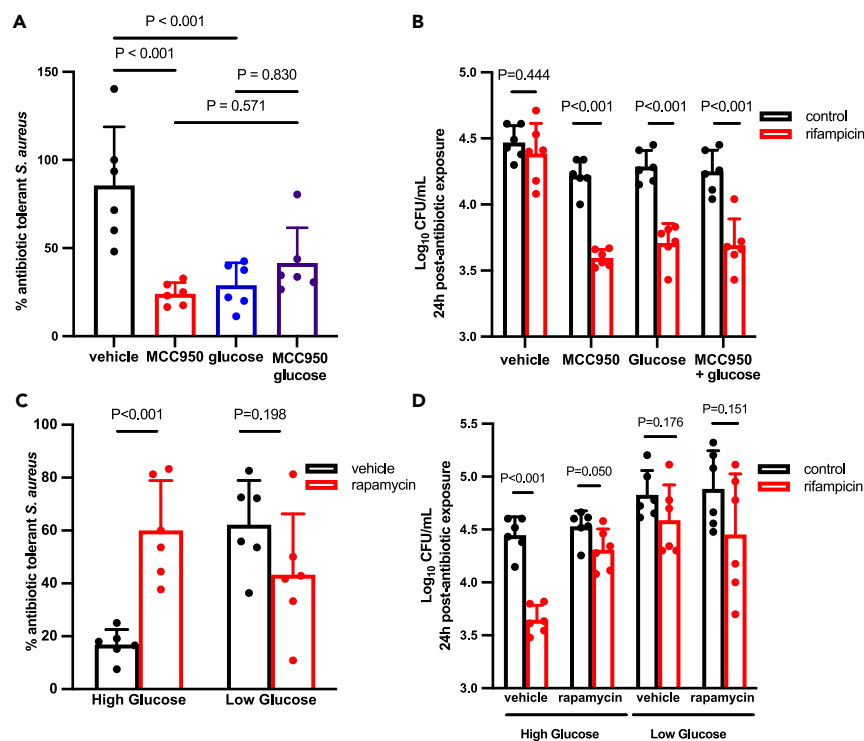


Figure 4. Glucose utilization is linked to antibiotic tolerance

(A and B) % rifampicin tolerance of *S. aureus* WT LAC in untreated or MCC950-treated BMDMs. BMDMs were infected at MOI 10 for 45 min, followed by addition of 50 μ g/ml gentamicin +/- 10 μ g/ml rifampicin. At 20hpi, 0.2% glucose was added to the extracellular media where indicated, followed by CFU enumeration at 24 h. % survival (A) was extrapolated from CFU/ml (B).

(C and D) BMDMs were cultured in DMEM (high glucose, 4.5 g/L) or MEM (low glucose, 1.0 g/L). Rapamycin-treated cells were incubated overnight in the presence of 100 ng/ml rapamycin. BMDMs were infected with WT LAC at MOI 10 for 45 min, followed by addition of 50 μ g/ml gentamicin +/- 10 μ g/ml rifampicin. % survival (C) was extrapolated from CFU/ml (D). See also Figure S4. Statistical significance was determined by using one-way ANOVA with Sidak's multiple comparison (A) or unpaired t-test (two-tailed) (B, C, and D). All experiments were performed in biological triplicate at least twice on two separate days ($n \geq 6$). Bars represent the mean +standard deviation.

infected with LAC_{lux} for 24 h. BMDMs were then lysed and relative luminescence (RLU) was measured in untreated and MCC950 treated. When NLRP3 was inhibited with MCC950, we observed increased ATP levels, which correlates with decreased antibiotic tolerance (Figure 3C).

Next, we determined if the addition of exogenous glucose could resuscitate and sensitize the cytoplasmic *S. aureus* antibiotic tolerant cells by stimulating *S. aureus* glycolysis. BMDMs were infected with WT LAC followed by treatment with or without rifampicin for 20 h. At 20hpi, 0.2% glucose (2 g/L; ~0.01 M) was added for 4 h, at which point macrophages were lysed and CFU enumerated. Addition of glucose decreased tolerance to rifampicin at a similar level observed with MCC950 treatment (Figures 4A and 4B). Treatment of the macrophages with both MCC950 and glucose did not result in any additional change in antibiotic susceptibility compared to single treatments (Figure 4A). This indicates that either blocking NLRP3-mediated activation of host cell glycolysis or addition of excess glucose is sufficient to sensitize antibiotic tolerant cells to rifampicin.

To further support the idea that glucose availability is a crucial determinant of antibiotic tolerance, we used rapamycin to repress glucose uptake by macrophages. Rapamycin selectively targets glucose uptake by host cells but not *S. aureus*, thus allowing us to interrogate how the altered microenvironment affects the formation of antibiotic tolerant cells. To capture the effect of rapamycin on glucose limitation, infected BMDMs were cultured in a high-glucose medium. In this scenario, we would expect fewer *S. aureus* antibiotic tolerant cells recovered from untreated BMDM due to the excess amount of glucose in the medium (4.5 g/L). Consistent with our hypothesis, we observed an increase in *S. aureus* antibiotic tolerant cells in macrophages treated with rapamycin in the high glucose media but not the low glucose media (Figures 4C and 4D). These data suggest that α -toxin-mediated NLRP3 activation leads to increased host cell glycolysis, depleting host cytosolic glucose levels, leading to increased antibiotic tolerant *S. aureus* due to nutrient deprivation. Together these data highlight the crucial role of glucose availability in antibiotic tolerance.

NLRP3 inhibition improves antibiotic efficacy in murine bacteremia

To determine if NLRP3 inhibition improves antibiotic efficacy *in vivo*, we examined antibiotic treatment outcome in a systemic *S. aureus* infection of WT mice pre-treated with MCC950. We chose to use the HG003 background for these studies as we have previously optimized

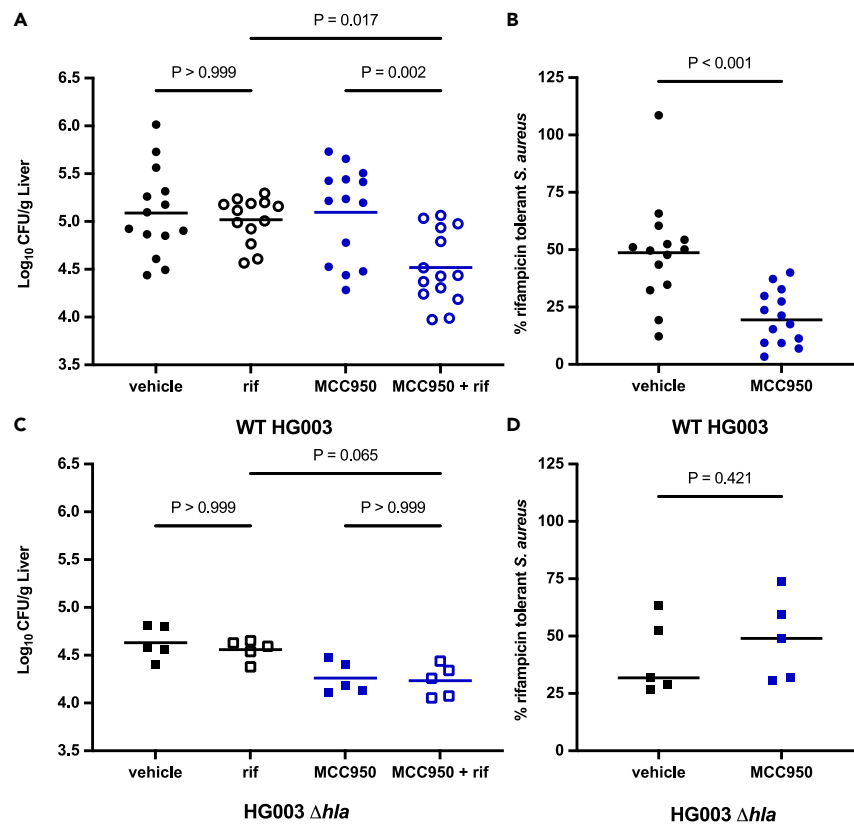


Figure 5. NLRP3 inhibition improves antibiotic efficacy against systemic *S. aureus* infection

(A and B) WT C57BL/6 mice were treated with 50 mg/kg MCC950 by ip injection, followed by tail vein iv infection with *S. aureus* strain HG003 1 h after treatment. At 24hpi, mice were administered 25 mg/kg rifampicin (rif) or vehicle control by ip injection.

(A) At 48hpi, *S. aureus* burden was enumerated in the liver. % antibiotic tolerant *S. aureus* (B) in vehicle versus MCC950-treated mice extrapolated from CFU/g (A). (C and D) WT C57BL/6 mice were treated as above and infected with HG003 Δhla . (C) At 48hpi, *S. aureus* burden was enumerated in the liver.

(D) % antibiotic tolerant *S. aureus* in vehicle versus MCC950-treated mice extrapolated from CFU/g (C). See also Figure S5. Each data point represents one mouse from three independent experiments (total n = 9 per group for WT alone infection and n = 5 for experiments with two strains).

(A and C) Statistical significance was determined using Kruskal-Wallis one-way ANOVA with Dunn's multiple comparison. Horizontal lines represent the mean. (B and D) Statistical significance was determined by the Mann-Whitney test. Horizontal lines represent the median. See also Figure S5.

systemic infection using this strain⁵ and the same antibiotic tolerance phenotype we see in LAC also occurs in HG003 (Figures S1C and S1D). Systemic infection was induced by tail vein intravenous (iv) injection of either WT HG003 (Figures 5A, 5B, S5A, and S5B) or HG003 Δhla (Figures 5C, 5D, S5C, and S5D), followed by treatment with rifampicin. MCC950 has a C_{max} of approximately 10 μ g/mL at a 3 mg/kg dose with an *in vivo* half-life of 3.27 h and it is inhibitory to NLRP3 at concentrations as low as 10 nM.⁴³ We therefore expected that the dose administered to the mice (50 mg/kg) will remain well above the inhibitory concentration throughout the experiment and this dose was previously demonstrated to inhibit inflammasome activation *in vivo*.⁴³ Mice treated with MCC950 prior to infection and treatment with rifampicin had significantly lower bacterial burdens in their livers (Figures 5A and 5B) and lower, although not significant, burden in their spleens (Figures S5A and S5B) relative to vehicle or rifampicin treated mice. Consistent with our tissue culture experiments, HG003 Δhla exhibited no change in tolerance to rifampicin when mice were treated with MCC950 (Figures 5C, 5B, S5C, and S5D). To verify that these data were not the result of acquired rifampicin resistance, organ homogenates were plated on solid media with and without rifampicin (Figure S5E). These data suggest that NLRP3 inhibition improves antibiotic treatment efficacy against systemic *S. aureus* infection.

DISCUSSION

S. aureus causes a variety of chronic and relapsing infections with high rates of antibiotic treatment failure, morbidity, and mortality. The metabolic versatility of *S. aureus* greatly contributes to its success as a pathogen. As a facultative anaerobe, *S. aureus* can colonize and proliferate in a variety of host niches. Inflammation-associated shifts in the host nutrient milieu alters *S. aureus* metabolic activity during infection.⁵³ Spatiotemporal variation in nutrient availability can cause bacteria to enter an antibiotic tolerant state.⁵⁴ As this and other studies demonstrate, the metabolic lifestyle of *S. aureus* in a given niche has significant impacts on antibiotic treatment efficacy, underpinning the importance of studying *S. aureus* antibiotic susceptibility in niche-specific contexts.⁵ We have previously identified the intracellular niche as a potent

driver of antibiotic tolerance in *S. aureus*, at least in part due to the ROS/RNS mediated collapse of the bacterial TCA cycle, resulting in reduced metabolism and ATP levels.^{5,6} Importantly, these studies were performed after 4 h of antibiotic treatment, with *S. aureus* remaining sequestered in the phagolysosome.⁵ In the current study, we examined the survival of *S. aureus* to antibiotics over 24 h, after the bacteria have escaped into the cytoplasm (Figure S4). We find an intricate link between NLRP3 inflammasome activation, host cell metabolism, and α -toxin wherein α -toxin activates NLRP3, increasing host cell glycolytic activity. Increased host cell glycolysis limits glucose availability for *S. aureus*, leading to cytoplasmic nutrient deprivation and subsequent tolerance. By blocking NLRP3 activation, we decrease antibiotic tolerance in *S. aureus* by stimulating *S. aureus* glycolysis.

NLRP3 activation is a two-signal process. Signal 1 is a priming step, typically TLR or other PRR recognition of PAMPs. Signal 2 can be a variety of different stimuli, including potassium ion efflux mediated by α -toxin, either directly or via packaging of *S. aureus* virulence factors in extracellular vesicles that are delivered to macrophages via endocytosis.^{20,39} TLR sensing of bacterial PAMPs, as well as NLRP3 activation, have been shown to shift macrophages to Warburg metabolism, characterized by increased glucose utilization and glycolytic flux.^{30–32,55,56} Additionally, α -toxin-mediated NLRP3 activation was recently shown to prevent immune clearance of *S. aureus* by recruiting mitochondria away from the phagolysosome, reducing mitochondrial ROS production and phagosomal acidification.¹³ Other studies have shown that antibody neutralization of α -toxin during *S. aureus* pneumonia infection facilitates immune clearance and prolongs the antibiotic treatment window,¹⁵ however inhibition of α -toxin by monoclonal antibodies did not improve outcomes in pulmonary *S. aureus* infections in humans.⁵⁷

This work further emphasizes that antibiotic efficacy is significantly determined by host cell activities at the site of infection. Importantly, these findings suggest that modulation of immune cell activities can improve antibiotic efficacy. Given the high rates of antibiotic treatment failure and mortality associated with *S. aureus* bacteremia, targeting the host immune response represents an important opportunity to improve treatment outcomes in patients.

Overall, our results identify a complex signaling network whereby interactions between the *S. aureus* virulence factor α -toxin and the NLRP3 inflammasome result in metabolic crosstalk between host and pathogen that profoundly impacts antibiotic treatment efficacy.

Limitations of the study

NLRP3 inflammasome activation has clearly been linked to *S. aureus* α -toxin,²⁰ however, other *S. aureus* virulence factors can also activate NLRP3. LukAB and PVL can act as signal 2 to induce inflammasome activation.²¹ Determining the contribution of other pore-forming toxins to antibiotic tolerance, through activation of the NLRP3 inflammasome, will be important in future studies. Additionally, NLRP3 activation is not the single contributor to *S. aureus* tolerance. We have previously shown at earlier timepoints ROS/RNS induces tolerance.^{5,6} It is possible further unexplored mechanisms act to induce antibiotic tolerance of intracellular *S. aureus*. This could explain the data with clinical isolates (Figure S3) where all isolates express α -toxin, but only half of them exhibited reduced tolerance when macrophages are pretreated with MCC950. Alternatively, the timing of phagosomal escape (and therefore exposure to cytoplasmic glucose) may be different between *S. aureus* strains, so we may have missed MCC950 induced tolerance at 24 h post-infection. There may also be variation in the timing of phagosomal escape between different host cells. We see NLRP3-mediated tolerance in human and mouse macrophage cells lines and mouse BMDM at 24 h post-infection. At this same timepoint we visualized WT *S. aureus* in the cytoplasm of J774A.1 cells (Figure S4). It will be important to investigate if timing of phagosomal escape and/or intracellular localization impacts antibiotic tolerance in other host cell types, such as primary human macrophages or neutrophils, or with other *S. aureus* strains.

As we investigated how NLRP3 activation affects antibiotic tolerance of intracellular *S. aureus*, this phenotype is limited to antibiotics that enter host cells. These assays cannot test tolerance to antibiotics that cannot enter the intercellular space, such as aminoglycosides and glycopeptides. Interestingly, *S. aureus* membrane-derived vesicles (MVs) can be internalized by macrophages, resulting in toxin-mediated activation of the NLRP3 inflammasome, without uptake of viable bacteria.³⁹ Activation of NLRP3 by extracellular *S. aureus* could potentially alter macrophage metabolism and glucose availability in the immediate extracellular space. It will be interesting to determine if inflammasome activation impacts extracellular glucose availability and consumption.

Lastly, while reliance of purified α -toxin in the Seahorse glycolysis assay directly assesses α -toxin mediated NLRP3 activation, impact(s) from other virulence factors could not be assessed. It is possible changes in macrophage glycolysis in response to *S. aureus* infection are different than those caused by α -toxin treatment alone.

STAR★METHODS

Detailed methods are provided in the online version of this paper and include the following:

- KEY RESOURCES TABLE
- RESOURCE AVAILABILITY
 - Lead contact
 - Materials availability
 - Data and code availability
- EXPERIMENTAL MODEL AND STUDY PARTICIPANT DETAILS
 - Animal model
 - BMDM isolation
 - THP-1 cell culture

- J774A.1 cell culture
- Bacterial strains and growth conditions
- **METHOD DETAILS**
 - BMDM infection
 - THP-1 cell culture and infection
 - ROS measurement
 - Minimum inhibitory concentration assay
 - Caspase-1 activity
 - LDH release assay
 - Western Blot
 - CellTiter-Blue viability assay
 - J774A.1 infection and microscopy
 - Glucose uptake assay
 - Seahorse XF Glycolysis Stress Assay
 - Relative ATP measurement
 - Murine bacteremia model
- **QUANTIFICATION AND STATISTICAL ANALYSIS**

SUPPLEMENTAL INFORMATION

Supplemental information can be found online at <https://doi.org/10.1016/j.isci.2023.107942>.

ACKNOWLEDGMENTS

This work was supported in part by NIH grants R01AI137273, R01AI173004 and a Burroughs Wellcome Fund investigator in the pathogenesis of infectious disease (PATH) award to B.P.C. The Microscopy Services Laboratory, Department of Pathology and Laboratory Medicine is supported in part by P30 CA016086 Cancer Center Core Support Grant to the UNC Lineberger Comprehensive Cancer Center. Seahorse assays were run by the Animal Metabolism and Phenotyping Core in the UNC Nutrition Obesity Research Center, which is supported by National Institute of Diabetes and Digestive and Kidney Diseases of the National Institutes of Health under Award Number P30DK056350. We thank Jovanka Voyitch for the α -toxin mutant strain, Roger Plaut for sharing JE2-lux (SAP430), Janelle Arthur for equipment, and Mark Ross for assistance with animal infections. We thank Jenny Ting, Lance Thurlow, Kim Walker, and Janelle Arthur for thoughtful discussions and Michelle Angeles-Solano for contributing to the graphical abstract. Graphical abstract was made using BioRender.

AUTHOR CONTRIBUTIONS

Conceptualization, B.P.C. and J.E.B.; Methodology, J.E.B., N.J.W., and B.P.C.; Investigation, J.E.B., N.J.W., K.L., J.B.P., and S.E.R.; Resources, B.P.C. and V.G.F.; Writing – Original Draft, J.E.B. and N.J.W.; Writing–Review and Editing, B.P.C., K.Y., J.B.P., and S.E.R., Visualization, J.E.B. and N.J.W.; Supervision, B.P.C.; Funding Acquisition, B.P.C.

DECLARATION OF INTERESTS

The authors declare no competing interests.

Received: January 31, 2023

Revised: June 27, 2023

Accepted: September 13, 2023

Published: September 17, 2023

REFERENCES

1. Cosgrove, S.E., Sakoulas, G., Perencevich, E.N., Schwaber, M.J., Karchmer, A.W., and Carmeli, Y. (2003). Comparison of mortality associated with methicillin-resistant and methicillin-susceptible *Staphylococcus aureus* bacteremia: a meta-analysis. *Clin. Infect. Dis.* 36, 53–59. <https://doi.org/10.1086/345476>.
2. Kourtis, A.P., Hatfield, K., Baggs, J., Mu, Y., See, I., Epton, E., Nadle, J., Kainer, M.A., Dumyati, G., Petit, S., et al. (2019). Vital Signs: Epidemiology and Recent Trends in Methicillin-Resistant and in Methicillin-Susceptible *Staphylococcus aureus* Bloodstream Infections - United States. *MMWR Morb. Mortal. Wkly. Rep.* 68, 214–219. <https://doi.org/10.15585/mmwr.mm6809e1>.
3. Labreche, M.J., Lee, G.C., Attridge, R.T., Mortensen, E.M., Koeller, J., Du, L.C., Nyren, N.R., Treviño, L.B., Treviño, S.B., Peña, J., et al. (2013). Treatment failure and costs in patients with methicillin-resistant *Staphylococcus aureus* (MRSA) skin and soft tissue infections: a South Texas Ambulatory Research Network (STARNet) study. *J. Am. Board Fam. Med.* 26, 508–517. <https://doi.org/10.3122/jabfm.2013.05.120247>.
4. Liu, J., Gefen, O., Ronin, I., Bar-Meir, M., and Balaban, N.Q. (2020). Effect of tolerance on the evolution of antibiotic resistance under drug combinations. *Science* 367, 200–204. <https://doi.org/10.1126/science.aay3041>.
5. Rowe, S.E., Wagner, N.J., Li, L., Beam, J.E., Wilkinson, A.D., Radlinski, L.C., Zhang, Q., Miao, E.A., and Conlon, B.P. (2020). Reactive oxygen species induce antibiotic tolerance during systemic *Staphylococcus aureus* infection. *Nat. Microbiol.* 5, 282–290. <https://doi.org/10.1038/s41564-019-0627-y>.
6. Beam, J.E., Wagner, N.J., Shook, J.C., Bahnsen, E.S.M., Fowler, V.G., Jr., Rowe, S.E.,

- and Conlon, B.P. (2021). Macrophage-produced peroxyne nitrite induces antibiotic tolerance and supersedes intrinsic mechanisms of persister formation. *Infect. Immun.* 89, IA10028621. <https://doi.org/10.1128/IAI.00286-21>.
7. Conlon, B.P., Rowe, S.E., Gandt, A.B., Nuxoll, A.S., Donegan, N.P., Zalis, E.A., Clair, G., Adkins, J.N., Cheung, A.L., and Lewis, K. (2016). Persister formation in *Staphylococcus aureus* is associated with ATP depletion. *Nat. Microbiol.* 1, 16051. <https://doi.org/10.1038/nmicrbiol.2016.51>.
8. Huemer, M., Mairpady Shambat, S., Bergada-Pijuan, J., Söderholm, S., Boumassoud, M., Vulin, C., Gómez-Mejía, A., Antelo Varela, M., Tripathi, V., Götschi, S., et al. (2021). Molecular reprogramming and phenotype switching in *Staphylococcus aureus* lead to high antibiotic persistence and affect therapy success. *Proc. Natl. Acad. Sci. USA* 118, e2014920118. <https://doi.org/10.1073/pnas.2014920118>.
9. Liu, Y., Tan, S., Huang, L., Abramovitch, R.B., Rohde, K.H., Zimmerman, M.D., Chen, C., Dartois, V., VanderVen, B.C., and Russell, D.G. (2016). Immune activation of the host cell induces drug tolerance in *Mycobacterium tuberculosis* both in vitro and in vivo. *J. Exp. Med.* 213, 809–825. <https://doi.org/10.1084/jem.20151248>.
10. Ronneau, S., Michaux, C., and Helaine, S. (2023). Decline in nitrosative stress drives antibiotic persister regrowth during infection. *Cell Host Microbe* 31, 993–1006.e6. <https://doi.org/10.1016/j.chom.2023.05.002>.
11. Vitko, N.P., Spahich, N.A., and Richardson, A.R. (2015). Glycolytic dependency of high-level nitric oxide resistance and virulence in *Staphylococcus aureus*. *mBio* 6, e00045-15. <https://doi.org/10.1128/mBio.00045-15>.
12. Fair, R.J., and Tor, Y. (2014). Antibiotics and bacterial resistance in the 21st century. *Perspect. Med. Chem.* 6, 25–64. <https://doi.org/10.4137/PMC.S14459>.
13. Cohen, T.S., Boland, M.L., Boland, B.B., Takahashi, V., Tovchigrechko, A., Lee, Y., Wilde, A.D., Mazaitis, M.J., Jones-Nelson, O., Tkaczyk, C., et al. (2018). *S. aureus* Evades Macrophage Killing through NLRP3-Dependent Effects on Mitochondrial Trafficking. *Cell Rep.* 22, 2431–2441. <https://doi.org/10.1016/j.celrep.2018.02.027>.
14. Kane, T.L., Car, Lee, S.W., et al. (2018). Virulence Factor Targeting of the Bacterial Pathogen *Staphylococcus aureus* for Vaccine and Therapeutics. *Curr. Drug Targets* 19, 111–127. <https://doi.org/10.2174/1389450117666161128123536>.
15. Hua, L., Cohen, T.S., Shi, Y., Datta, V., Hilliard, J.J., Tkaczyk, C., Suzich, J., Stover, C.K., and Sellman, B.R. (2015). MEDI4893* Promotes Survival and Extends the Antibiotic Treatment Window in a *Staphylococcus aureus* Immunocompromised Pneumonia Model. *Antimicrob. Agents Chemother.* 59, 4526–4532. <https://doi.org/10.1128/AAC.00510-15>.
16. Vu, T.T.T., Nguyen, N.T.Q., Tran, V.G., Gras, E., Mao, Y., Jung, D.H., Tkaczyk, C., Sellman, B.R., and Diep, B.A. (2020). Protective Efficacy of Monoclonal Antibodies Neutralizing Alpha-Hemolysin and Bicomponent Leukocidins in a Rabbit Model of *Staphylococcus aureus* Necrotizing Pneumonia. *Antimicrob. Agents Chemother.* 64, e02220-19. <https://doi.org/10.1128/AAC.02220-19>.
17. Howden, B.P., Giulieri, S.G., Wong Fok Lung, T., Baines, S.L., Sharkey, L.K., Lee, J.Y.H., Hachani, A., Monk, I.R., and Steiner, T.P. (2023). *Staphylococcus aureus* host interactions and adaptation. *Nat. Rev. Microbiol.* 21, 380–395. <https://doi.org/10.1038/s41579-023-00852-y>.
18. Kebaier, C., Chamberland, R.R., Allen, I.C., Gao, X., Broglie, P.M., Hall, J.D., Jania, C., Doerschuk, C.M., Tilley, S.L., and Duncan, J.A. (2012). *Staphylococcus aureus* alpha-hemolysin mediates virulence in a murine model of severe pneumonia through activation of the NLRP3 inflammasome. *J. Infect. Dis.* 205, 807–817. <https://doi.org/10.1093/infdis/jir846>.
19. Kitur, K., Parker, D., Nieto, P., Ahn, D.S., Cohen, T.S., Chung, S., Wachtel, S., Bueno, S., and Prince, A. (2015). Toxin-induced necroptosis is a major mechanism of *Staphylococcus aureus* lung damage. *PLoS Pathog.* 11, e1004820. <https://doi.org/10.1371/journal.ppat.1004820>.
20. Craven, R.R., Gao, X., Allen, I.C., Gris, D., Bubeck-Wardenburg, J., McElvania-Tekippe, E., Ting, J.P., and Duncan, J.A. (2009). *Staphylococcus aureus* alpha-hemolysin activates the NLRP3-inflammasome in human and mouse monocytic cells. *PLoS One* 4, e7446. <https://doi.org/10.1371/journal.pone.0007446>.
21. Melehan, J.H., and Duncan, J.A. (2016). Inflammasome Activation Can Mediate Tissue-Specific Pathogenesis or Protection in *Staphylococcus aureus* Infection. *Curr. Top. Microbiol. Immunol.* 397, 257–282. https://doi.org/10.1007/978-3-319-41171-2_13.
22. Tkaczyk, C., Jones-Nelson, O., Shi, Y.Y., Tabor, D.E., Cheng, L., Zhang, T., and Sellman, B.R. (2022). Neutralizing *Staphylococcus aureus* Virulence with AZD6389, a Three mAb Combination, Accelerates Closure of a Diabetic Polymicrobial Wound. *mSphere* 7, e0013022. <https://doi.org/10.1128/msphere.00130-22>.
23. Ortines, R.V., Liu, H., Cheng, L.I., Cohen, T.S., Lawlor, H., Gami, A., Wang, Y., Dillen, C.A., Archer, N.K., Miller, R.J., et al. (2018). Neutralizing Alpha-Toxin Accelerates Healing of *Staphylococcus aureus*-Infected Wounds in Nondiabetic and Diabetic Mice. *Antimicrob. Agents Chemother.* 62, e02288-17. <https://doi.org/10.1128/AAC.02288-17>.
24. Duan, L., Zhang, J., Chen, Z., Gou, Q., Xiong, Q., Yuan, Y., Jing, H., Zhu, J., Ni, L., Zheng, Y., et al. (2021). Antibiotic Combined with Epitope-Specific Monoclonal Antibody Cocktail Protects Mice Against Bacteremia and Acute Pneumonia from Methicillin-Resistant *Staphylococcus aureus* Infection. *J. Inflamm. Res.* 14, 4267–4282. <https://doi.org/10.2147/JIR.S325286>.
25. Miller, L.S., Fowler, V.G., Shukla, S.K., Rose, W.E., and Proctor, R.A. (2020). Development of a vaccine against *Staphylococcus aureus* invasive infections: Evidence based on human immunity, genetics and bacterial evasion mechanisms. *FEMS Microbiol. Rev.* 44, 123–153. <https://doi.org/10.1093/femsre/fuz030>.
26. Maher, B.M., Mulcahy, M.E., Murphy, A.G., Wilk, M., O'Keefe, K.M., Geoghegan, J.A., Lavelle, E.C., and McLoughlin, R.M. (2013). Nlrp3-driven interleukin 17 production by gamma-delta T cells controls infection outcomes during *Staphylococcus aureus* surgical site infection. *Infect. Immun.* 81, 4478–4489. <https://doi.org/10.1128/IAI.01026-13>.
27. Cho, J.S., Guo, Y., Ramos, R.I., Hebroni, F., Plaisier, S.B., Xuan, C., Granick, J.L., Matsushima, H., Takashima, A., Iwakura, Y., et al. (2012). Neutrophil-derived IL-1beta is sufficient for abscess formation in immunity against *Staphylococcus aureus* in mice. *PLoS Pathog.* 8, e1003047. <https://doi.org/10.1371/journal.ppat.1003047>.
28. Liu, R., Liu, Y., Liu, C., Gao, A., Wang, L., Tang, H., Wu, Q., Wang, X., Tian, D., Qi, Z., and Shen, Y. (2021). NEK7-Mediated Activation of NLRP3 Inflammasome Is Coordinated by Potassium Efflux/Syk/JNK Signaling During *Staphylococcus aureus* Infection. *Front. Immunol.* 12, 747370. <https://doi.org/10.3389/fimmu.2021.747370>.
29. Liu, C., Hao, K., Liu, Z., Liu, Z., and Guo, N. (2021). Epigallocatechin gallate (EGCG) attenuates staphylococcal alpha-hemolysin (Hla)-induced NLRP3 inflammasome activation via ROS-MAPK pathways and EGCG-Hla interactions. *Int. Immunopharm.* 100, 108170. <https://doi.org/10.1016/j.intimp.2021.108170>.
30. Finucane, O.M., Sugrue, J., Rubio-Araiz, A., Guillot-Sestier, M.V., and Lynch, M.A. (2019). The NLRP3 inflammasome modulates glycolysis by increasing PFKFB3 in an IL-1beta-dependent manner in macrophages. *Sci. Rep.* 9, 4034. <https://doi.org/10.1038/s41598-019-40619-1>.
31. Sanman, L.E., Qian, Y., Eisele, N.A., Ng, T.M., van der Linden, W.A., Monack, D.M., Weerapana, E., and Bogoy, M. (2016). Disruption of glycolytic flux is a signal for inflammasome signaling and pyroptotic cell death. *Elife* 5, e13663. <https://doi.org/10.7554/eLife.13663>.
32. Shao, W., Yeretssian, G., Doiron, K., Hussain, S.N., and Saleh, M. (2007). The caspase-1 digestome identifies the glycolysis pathway as a target during infection and septic shock. *J. Biol. Chem.* 282, 36321–36329. <https://doi.org/10.1074/jbc.M708182200>.
33. Yu, Q., Guo, M., Zeng, W., Zeng, M., Zhang, X., Zhang, Y., Zhang, W., Jiang, X., and Yu, B. (2022). Interactions between NLRP3 inflammasome and glycolysis in macrophages: New insights into chronic inflammation pathogenesis. *Inflamm. Dis.* 10, e581. <https://doi.org/10.1002/iid3.581>.
34. Acocella, G., Carlone, N.A., Cuffini, A.M., and Cavallo, G. (1985). The penetration of rifampicin, pyrazinamide, and pyrazinoic acid into mouse macrophages. *Am. Rev. Respir. Dis.* 132, 1268–1273. <https://doi.org/10.1164/arrd.1985.132.6.1268>.
35. Barcia-Macay, M., Seral, C., Mingeot-Leclercq, M.P., Tulkens, P.M., and Van Bambeke, F. (2006). Pharmacodynamic evaluation of the intracellular activities of antibiotics against *Staphylococcus aureus* in a model of THP-1 macrophages. *Antimicrob. Agents Chemother.* 50, 841–851. <https://doi.org/10.1128/AAC.50.3.841-851.2006>.
36. Jung, Y.J., Koh, Y., Hong, S.B., Chung, J.W., Ho Choi, S., Kim, N.J., Kim, M.N., Choi, I.S., Han, S.Y., Kim, W.D., et al. (2010). Effect of vancomycin plus rifampicin in the treatment of nosocomial methicillin-resistant *Staphylococcus aureus* pneumonia. *Crit. Care Med.* 38, 175–180. <https://doi.org/10.1097/ccm.0b013e3181b9ecce>.
37. Park, H.M., Yoo, H.S., Oh, T.H., Kim, D., and Han, H.R. (1999). Immunogenicity of alpha-toxin, capsular polysaccharide (CPS) and recombinant fibronectin-binding protein (r-FnBP) of *Staphylococcus aureus* in rabbit.

- J. Vet. Med. Sci. 61, 995–1000. <https://doi.org/10.1292/jvms.61.995>.
38. Rios, N., Piacenza, L., Trujillo, M., Martínez, A., Demicheli, V., Prolo, C., Álvarez, M.N., López, G.V., and Radi, R. (2016). Sensitive detection and estimation of cell-derived peroxynitrite fluxes using fluorescein-boronate. *Free Radic. Biol. Med.* 101, 284–295. <https://doi.org/10.1016/j.freeradbiomed.2016.08.033>.
 39. Wang, X., Eagen, W.J., and Lee, J.C. (2020). Orchestration of human macrophage NLRP3 inflammasome activation by Staphylococcus aureus extracellular vesicles. *Proc. Natl. Acad. Sci. USA* 117, 3174–3184. <https://doi.org/10.1073/pnas.1915829117>.
 40. Muñoz-Planillo, R., Kuffa, P., Martínez-Colón, G., Smith, B.L., Rajendiran, T.M., and Núñez, G. (2013). K(+) efflux is the common trigger of NLRP3 inflammasome activation by bacterial toxins and particulate matter. *Immunity* 38, 1142–1153. <https://doi.org/10.1016/j.immuni.2013.05.016>.
 41. Aachoui, Y., Sagulenko, V., Miao, E.A., and Stacey, K.J. (2013). Inflammasome-mediated pyroptotic and apoptotic cell death, and defense against infection. *Curr. Opin. Microbiol.* 16, 319–326. <https://doi.org/10.1016/j.mib.2013.04.004>.
 42. Miller, L.S., Pietras, E.M., Uricchio, L.H., Hirano, K., Rao, S., Lin, H., O’Connell, R.M., Wakura, Y., Cheung, A.L., Cheng, G., and Modlin, R.L. (2007). Inflammasome-mediated production of IL-1 β is required for neutrophil recruitment against Staphylococcus aureus in vivo. *J. Immunol.* 179, 6933–6942. <https://doi.org/10.4049/jimmunol.179.10.6933>.
 43. Coll, R.C., Robertson, A.A.B., Chae, J.J., Higgins, S.C., Muñoz-Planillo, R., Inserra, M.C., Vetter, I., Dungan, L.S., Monks, B.G., Stutz, A., et al. (2015). A small-molecule inhibitor of the NLRP3 inflammasome for the treatment of inflammatory diseases. *Nat. Med.* 21, 248–255. <https://doi.org/10.1038/nm.3806>.
 44. Perera, A.P., Fernando, R., Shinde, T., Gundamaraju, R., Southam, B., Sohal, S.S., Robertson, A.A.B., Schroder, K., Kunde, D., and Eri, R. (2018). MCC950, a specific small molecule inhibitor of NLRP3 inflammasome attenuates colonic inflammation in spontaneous colitis mice. *Sci. Rep.* 8, 8618. <https://doi.org/10.1038/s41598-018-26775-w>.
 45. Kovarova, M., Hesker, P.R., Jania, L., Nguyen, M., Snouwaert, J.N., Xiang, Z., Lommatzsch, S.E., Huang, M.T., Ting, J.P.Y., and Koller, B.H. (2012). NLRP1-dependent pyroptosis leads to acute lung injury and morbidity in mice. *J. Immunol.* 189, 2006–2016. <https://doi.org/10.4049/jimmunol.1201065>.
 46. Münzenmayer, L., Geiger, T., Daiber, E., Schulte, B., Autenrieth, S.E., Fraunholz, M., and Wolz, C. (2016). Influence of Sae-regulated and Agr-regulated factors on the escape of Staphylococcus aureus from human macrophages. *Cell Microbiol.* 18, 1172–1183. <https://doi.org/10.1111/cmi.12577>.
 47. Lu, K.Y., Wagner, N.J., Velez, A.Z., Ceppe, A., Conlon, B.P., and Muhlebach, M.S. (2023). Antibiotic Tolerance and Treatment Outcomes in Cystic Fibrosis Methicillin-Resistant Staphylococcus aureus Infections. *Microbiol. Spectr.* 11, e0406122. <https://doi.org/10.1128/spectrum.04061-22>.
 48. Sharma-Kuinkel, B.K., Wu, Y., Tabor, D.E., Mok, H., Sellman, B.R., Jenkins, A., Yu, L., Jafri, H.S., Rude, T.H., Ruffin, F., et al. (2015). Characterization of alpha-toxin hla gene variants, alpha-toxin expression levels, and levels of antibody to alpha-toxin in hemodialysis and postsurgical patients with Staphylococcus aureus bacteremia. *J. Clin. Microbiol.* 53, 227–236. <https://doi.org/10.1128/JCM.02023-14>.
 49. Herbert, S., Ziebandt, A.K., Ohlsen, K., Schäfer, T., Hecker, M., Albrecht, D., Novick, R., and Götz, F. (2010). Repair of global regulators in Staphylococcus aureus 8325 and comparative analysis with other clinical isolates. *Infect. Immun.* 78, 2877–2889. <https://doi.org/10.1128/IAI.00088-10>.
 50. Bravo-Santano, N., Ellis, J.K., Mateos, L.M., Calle, Y., Keun, H.C., Behrends, V., and Letek, M. (2018). Intracellular Staphylococcus aureus Modulates Host Central Carbon Metabolism To Activate Autophagy. *mSphere* 3, e00374-18. <https://doi.org/10.1128/mSphere.00374-18>.
 51. Jarry, T.M., Memmi, G., and Cheung, A.L. (2008). The expression of alpha-haemolysin is required for Staphylococcus aureus phagosomal escape after internalization in CFT-1 cells. *Cell Microbiol.* 10, 1801–1814. <https://doi.org/10.1111/j.1462-5822.2008.01166.x>.
 52. Xu, T., Ripp, S., Saylor, G.S., and Close, D.M. (2014). Expression of a humanized viral 2A-mediated lux operon efficiently generates autonomous bioluminescence in human cells. *PLoS One* 9, e96347. <https://doi.org/10.1371/journal.pone.0096347>.
 53. Potter, A.D., Butrico, C.E., Ford, C.A., Curry, J.M., Trenary, I.A., Tummarakota, S.S., Hendrix, A.S., Young, J.D., and Cassat, J.E. (2020). Host nutrient milieu drives an essential role for aspartate biosynthesis during invasive Staphylococcus aureus infection. *Proc. Natl. Acad. Sci. USA* 117, 12394–12401. <https://doi.org/10.1073/pnas.1922211117>.
 54. Moreno-Gómez, S., Dal Co, A., van Vliet, S., and Ackermann, M. (2021). Microfluidics for Single-Cell Study of Antibiotic Tolerance and Persistence Induced by Nutrient Limitation. *Methods Mol. Biol.* 2357, 107–124. https://doi.org/10.1007/978-1-0716-1621-5_8.
 55. Shi, L., Salamon, H., Eugenin, E.A., Pine, R., Cooper, A., and Gennaro, M.L. (2015). Infection with Mycobacterium tuberculosis induces the Warburg effect in mouse lungs. *Sci. Rep.* 5, 18176. <https://doi.org/10.1038/srep18176>.
 56. Rother, M., Teixeira da Costa, A.R., Zietlow, R., Meyer, T.F., and Rudel, T. (2019). Modulation of Host Cell Metabolism by Chlamydia trachomatis. *Microbiol. Spectr.* 7. <https://doi.org/10.1128/microbiolspec.BA1-0012-2019>.
 57. François, B., Jafri, H.S., Chastre, J., Sánchez-García, M., Eggmann, P., Dequin, P.F., Huberlant, V., Vina Viña Soria, L., Boulain, T., Bretonnière, C., et al. (2021). Efficacy and safety of suvatroxumab for prevention of Staphylococcus aureus ventilator-associated pneumonia (SAATELLITE): a multicentre, randomised, double-blind, placebo-controlled, parallel-group, phase 2 pilot trial. *Lancet Infect. Dis.* 21, 1313–1323. [https://doi.org/10.1016/S1473-3099\(20\)30995-6](https://doi.org/10.1016/S1473-3099(20)30995-6).
 58. Amend, S.R., Valkenburg, K.C., and Pienta, K.J. (2016). Murine Hind Limb Long Bone Dissection and Bone Marrow Isolation. *J. Vis. Exp.* <https://doi.org/10.3791/53936>.
 59. Nygaard, T.K., Pallister, K.B., DuMont, A.L., DeWald, M., Watkins, R.L., Pallister, E.Q., Malone, C., Griffith, S., Horswill, A.R., Torres, V.J., and Voyich, J.M. (2012). Alpha-toxin induces programmed cell death of human T cells, B cells, and monocytes during USA300 infection. *PLoS One* 7, e36532. <https://doi.org/10.1371/journal.pone.0036532>.
 60. Kolaczowska, E., Jenne, C.N., Surewaard, B.G.J., Thanabalasuriar, A., Lee, W.Y., Sanz, M.J., Mowen, K., Opendakker, G., and Kubes, P. (2015). Molecular mechanisms of NET formation and degradation revealed by intravital imaging in the liver vasculature. *Nat. Commun.* 6, 6673. <https://doi.org/10.1038/ncomms7673>.
 61. Liu, H., Archer, N.K., Dillen, C.A., Wang, Y., Ashbaugh, A.G., Ortines, R.V., Kao, T., Lee, S.K., Cai, S.S., Miller, R.J., et al. (2017). Staphylococcus aureus Epicutaneous Exposure Drives Skin Inflammation via IL-36-Mediated T Cell Responses. *Cell Host Microbe* 22, 653–666.e5. <https://doi.org/10.1016/j.chom.2017.10.006>.
 62. Peyrusson, F., Varet, H., Nguyen, T.K., Legendre, R., Sismeiro, O., Coppée, J.Y., Wolz, C., Tenson, T., and Van Bambeke, F. (2020). Intracellular Staphylococcus aureus persists upon antibiotic exposure. *Nat. Commun.* 11, 2200. <https://doi.org/10.1038/s41467-020-15966-7>.
 63. Schneider, C.A., Rasband, W.S., and Eliceiri, K.W. (2012). NIH Image to ImageJ: 25 years of image analysis. *Nat. Methods* 9, 671–675. <https://doi.org/10.1038/nmeth.2089>.
 64. Sage, D., Donati, L., Soulez, F., Fortun, D., Schmit, G., Seitz, A., Guiet, R., Vonesch, C., and Unser, M. (2017). DeconvolutionLab2: An open-source software for deconvolution microscopy. *Methods* 115, 28–41. <https://doi.org/10.1016/j.jymeth.2016.12.015>.

STAR★METHODS

KEY RESOURCES TABLE

REAGENT or RESOURCE	SOURCE	IDENTIFIER
Antibodies		
Anti-alpha-hemolysin antibody [8B7]	Abcam	Cat# ab190467
Goat anti-mouse HRP	Cayman Chemical	Cat# 10004302, RRID: AB_10078261
Bacterial and virus strains		
LAC	Nygaard et al. ⁵⁹	BC1520
LAC Δhla	Nygaard et al. ⁵⁹	BC1521
LAC Δhla phla	Nygaard et al. ⁵⁹	BC1522
HG003	Herbert et al. ⁴⁹	BC1
HG003 Δhla	This study	BC1546
LAC <i>luxABDCE</i>	This study	BC1563
LAC GFP	Kolaczowska et al. ⁶⁰	BC47
BC1263	Beam et al. ⁶	BC1263
BC1264	Beam et al. ⁶	BC1264
BC1267	Beam et al. ⁶	BC1267
BC1274	Beam et al. ⁶	BC1274
Chemicals, peptides, and recombinant proteins		
MCC950 (used in <i>in vitro</i> studies)	Cayman Chemical	Cat# 17510
MCC950 sodium salt (used in animal model)	Selleckchem	Cat# S7809
Alpha toxin	Sigma	Cat# H939
Rapamycin	Thermo Scientific	Cat# J62473MF
Oridonin	Cayman Chemical	Cat# 25665
Rifampicin	Fisher Biochemicals	Cat# BP2679
Vancomycin	Cayman Chemical	Cat# 15327
Moxifloxacin	Thermo Scientific	Cat# 457960010
Gentamicin	Gibco	Cat# 15750060
Dulbecco's Modified Eagle Medium (DMEM)	Gibco	Cat# 11995065
Minimum Essential Media (MEM)	Gibco	Cat# 11095080
Roswell Park Memorial Institute (RPMI) 1640	Gibco	Cat# 11875093
Critical commercial assays		
Caspase-Glo 1 Inflammasome Assay	Promega	Cat# G9951
LDH-Glo Cytotoxicity Assay	Promega	Cat# J2380
CellTiter-Blue Cell Viability Assay	Promega	Cat# G8080
Glucose Uptake-Glo	Promega	Cat# J1341
Seahorse XF Glycolysis Stress Test Kit	Agilent	Cat# 103020-100
Deposited data		
Prism files for Figures	Mendeley	https://data.mendeley.com/datasets/6msmhr9vrs/1 https://doi.org/10.17632/6msmhr9vrs.2
Experimental models: Cell lines		
J774A.1	UNC TCF	RRID:CVCL_4692
THP-1	UNC TCF	RRID:CVCL_0006

(Continued on next page)

Continued

REAGENT or RESOURCE	SOURCE	IDENTIFIER
<i>Experimental models: Organisms/strains</i>		
Mouse: C57BL/6	Jackson Labs	RRID:IMSR_JAX:000664
Mouse: B6.129S6-Nlrp3 ^{tm1Bhk}	Jackson Labs	RRID:IMSR_JAX:021302
<i>Software and algorithms</i>		
ImageJ	Schneider et al. ⁶³	https://imagej.nih.gov
ImageJ Plug In: DeconvolutionLab2	Sage et al. ⁶⁴	http://bigwww.epfl.ch/deconvolution/deconvolutionlab2/
GraphPad Prism	GraphPad Software	RRID:SCR_002798
BioRender	BioRender	RRID:SCR_018361

RESOURCE AVAILABILITY

Lead contact

Additional information and requests for resources of reagents should be directed to and will be fulfilled by the lead contact, Brian Conlon (Brian_Conlon@med.unc.edu).

Materials availability

This study did not generate any new reagents.

Data and code availability

- Raw data used to generate Figures were deposited on Mendeley and are publicly available at Mendeley Data: <https://doi.org/10.17632/6msmhr9vrs.2>.
- This paper does not contain original code.
- Any additional information required to reanalyze the data reported in this paper is available from the [lead contact](#) upon request.

EXPERIMENTAL MODEL AND STUDY PARTICIPANT DETAILS

Animal model

All protocols used in this study were approved by the Institutional Animal Care and Use Committees at the University of North Carolina at Chapel Hill and met guidelines of the US National Institutes of Health for the humane care of animals. WT C57BL/6J (Jackson #000664) and NLRP3^{-/-} (B6.129S6-Nlrp3^{tm1Bhk}, Jackson #021302)⁴⁵ mice were housed 2–5 animals per cage in a pathogen-specific free facility with *ad libitum* access to food and water. Animals were randomly assigned to experimental groups.

BMDM isolation

Bone marrow from 6 to 20 week old WT male and female C57BL/6J mice or 10 week old female mice lacking NLRP3 (B6.129S6-Nlrp3^{tm1Bhk}) was isolated as described in Amend et al.⁵⁸ Bone marrow cells were differentiated for 7 days in Dulbecco's Modified Eagle Medium (DMEM, Gibco) + 10% FBS + L-glutamine + sodium pyruvate + sodium bicarbonate +30% L929-conditioned media. After 7 days in DMEM with L929-condition media, BMDM were cultured in minimum essential media (MEM, Gibco) + 10% FBS + L-glutamine (complete MEM) or DMEM +10% FBS + L-glutamine + non-essential amino acids + sodium pyruvate (complete DMEM) at 37°C, 5% CO₂.

THP-1 cell culture

THP-1 monocyte-like cells (RRID:CVCL_0006) were cultured in RPMI-1640 (Gibco) + 10% FBS + L-glutamine (complete RPMI) at 37°C, 5% CO₂. For differentiation into macrophages, THP-1 cells were seeded at 4x10⁵ cells/ml in complete RPMI +20 ng/ml phorbol 12-myristate 13-acetate (PMA) for 24 h. The THP-1 cell line was derived from cells from a 1 year old male child. We did not authenticate the cell line.

J774A.1 cell culture

J774A.1 murine macrophage-like cells (RRID:CVCL_4692) were cultured in complete DMEM as described above. Cells were cultured overnight in complete MEM at 37°C, 5% CO₂ prior to infection with *S. aureus*. J774A.1 cells were isolated from an adult female BALB/cN mouse. We did not authenticate the cell line.

Bacterial strains and growth conditions

S. aureus strains LAC (USA300), LAC Δhla ⁵⁹, LAC $\Delta hla phla$ ⁵⁹, LACluxABDCE, HG003^{11,49}, HG003 Δhla , and LAC GFP⁶⁰ were routinely cultured in Mueller Hinton broth (MHB) at 37°C and 225 r.p.m. Δhla strains were grown in the presence of 250 µg/ml spectinomycin and the complementation strain in 250 µg/ml spectinomycin +20 µg/ml chloramphenicol. LACluxABDCE was grown in MHB with 10 µg/ml chloramphenicol. LACluxABDCE was created via phage transduction of the *lux* cassette from JE2luxABDCE.⁶¹

METHOD DETAILS

BMDM infection

Bone marrow derived macrophage cells were plated at 4×10^5 cells/ml in complete MEM complete DMEM and allowed to adhere overnight at 37°C, 5% CO₂. Cells were either plated at 0.5 mL/well in 24 well plates or 100 µL/well in 96 well plates. For assays with MCC950 and oridonin, BMDMs were primed for 4 h with 10 ng/ml lipopolysaccharide (LPS, a potent signal 1 for NLRP3 activation) to ensure macrophages received a robust signal 1 prior to inhibitor treatment, followed by 30 min treatment with 10 µM MCC950 in serum-free media or 5 µM oridonin. Where indicated, BMDMs were treated with 100 ng/ml rapamycin overnight. BMDMs were incubated with *S. aureus* LAC, LAC Δhla , LAC $\Delta hla phla$, HG003, or HG003 Δhla , at MOI 10. Tissue culture plates were spun at 500xg for 5 min then incubated for 45 min at 37°C, 5% CO₂ to allow for internalization of bacteria. Media was removed, cells were washed 1x with PBS, and media was replaced with complete MEM or DMEM +50-µg/ml gentamicin. 10 µg/ml rifampicin and/or 50 µg/ml vancomycin or 3 µg/ml moxifloxacin were added as indicated.^{6,62} For glucose sensitization experiments (Figures 4C and 4D), 0.2% (2g/L, ~0.01 M) glucose was added at 20hpi. At indicated timepoints, media was removed, cells were washed 3x with PBS and macrophages were lysed with 1% Triton X-100. CFU were enumerated via dilution plating on tryptic soy agar (TSA) plates. All experiments were performed in biological triplicate (n = 3) at least twice on two separate days (total n \geq 6). Statistical significance was calculated using unpaired t-test (two-tailed) or one-way ANOVA with Sidak's multiple comparison as described in the Figure legends.

THP-1 cell culture and infection

After 24 h of differentiation to macrophages in RPMI+PMA, THP-1 cells were weaned in complete MEM for 1 h. Cells were infected as BMDM above. Experiments were performed in biological triplicate (n = 3) on two separate days (total n = 6). Statistical significance was calculated using unpaired t-test (two-tailed) or one-way ANOVA with Sidak's multiple comparison as described in the Figure legends.

ROS measurement

The luminescent probe L-012 (Wako Chemical Corporation) and fluorescein-boronate fluorescent (FI-B) probe were used to measure ROS. BMDMs were plated at 4×10^4 cells per well in white tissue-culture-treated 96-well plates. For L-012, the cells were washed three times with PBS. L-012 was diluted to 150 µM in Hanks' balanced salt solution (Gibco). Luminescence was read immediately using a Biotek Synergy H1 microplate reader. For FI-B, 25 µM FI-B was added and fluorescence was read at 492 nm/515 nm (excitation/emission) using the plate reader as above. Data shown are representative of 2 independent assays of 3 biological replicates. Statistical significance was calculated using unpaired t-test (two-tailed).

Minimum inhibitory concentration assay

The mutant strain Δhla and its parental strain LAC were cultured in Mueller–Hinton broth containing serially diluted rifampicin (0–0.2 µg/mL), moxifloxacin (0–10 µg/mL) or vancomycin (0–16 µg/mL) in 96-well assay plates (Costar) at 37°C for 16–24 h. The MICs were determined by the absence of bacterial growth. Three independent assays, each with biological triplicates, were performed to ensure the reproducibility (n = 9).

Caspase-1 activity

Caspase-1 activity was measured in BMDMs infected with LAC or LAC Δhla at MOI 10 as above. After 1 h, 50 µg/ml gentamicin was added, and cells were incubated for 24 h. At 24 h, caspase-1 activity was measured using the Caspase-Glo 1 Inflammasome Assay kit (Promega) per manufacturer's instructions. Experiments were performed in biological triplicate twice on two separate days (n = 6). Statistical significance was determined by unpaired t-test (two-tailed).

LDH release assay

Untreated or MCC950-treated BMDMs were infected at MOI 10 for 1 h with *S. aureus* LAC or LAC Δhla as above. After 1 h, 50 µg/ml gentamicin was added, and cells were incubated for 24 h. At 24 h, lactate dehydrogenase in the culture medium was measured by the LDH-Glo Assay Kit (Promega) per manufacturer's instructions. Experiments were performed in biological triplicate twice on two separate days (n = 6). Statistical significance was determined by unpaired t-test (two-tailed).

Western Blot

Supernatant from stationary phase cultures of *S. aureus* were concentrated using a Amicon Ultra 10 kDa spin filter (Millipore). Protein was quantified by Bio-Rad colorimetric protein assay and 50 µg of each sample was loaded onto a 4–12% gradient gel (Invitrogen). Proteins

were transferred to PVDF membrane (Thermo Scientific) and stained with Ponceau S (Sigma) to check transfer. Membrane was blocked for 1 h in TBST (TBS+ 0.1% tween 20) + 5% BSA at room temperature. Anti α -toxin antibody (Abcam, clone 8B7) was incubated at 1 μ g/ml in TBST+1% BSA overnight at 4°C. Membrane was washed with TBST 3x followed by 1 h incubation with goat anti-mouse HRP (Cayman) at 1:5,000 in TBST+1% BSA. After washing, ECL Clarity substrate (Bio-Rad) was added to the membrane and signal was detected on G-Box Chemi XX6 imager (Syngene). Western blotting was repeated with a second set of biological samples to verify results (n = 2).

CellTiter-Blue viability assay

Untreated or MCC950-treated BMDMs cultured in black 96 well plates were infected at MOI 10 for 1 h with *S. aureus* LAC as above. After 1 h, 50 μ g/ml gentamicin was added, and cells were incubated for 24 h. At 24 h CellTiter-Blue Assay reagent (Promega) was used to measure macrophage viability following the manufactures instructions. Briefly, 20 μ L of reagent was added to each well (100 μ L culture) and mixed. Fluorescence was read at 570 nm on a Biotek Synergy H1 microplate reader. Experiments were performed in biological triplicate twice on two separate days (n = 6). Statistical significance was determined using a one-way ANOVA with Sidak's multiple comparison.

J774A.1 infection and microscopy

J774A.1 cells were seeded at a density of 2×10^5 per well on poly-L-lysine coated number 1.5 glass coverslips in 24 well plates. Cells were primed with 5 μ g/mL LPS for 1 h before being infected with wild type LAC expressing GFP (LAC-GFP)⁶⁰ at an MOI of 10. One-hour post-infection (hpi), cells were washed 1x in PBS and media was replaced with MEM supplemented with 10 μ g/ml lysostaphin. One hour prior to harvest, LysoTracker red (Invitrogen) was added to indicated samples at 100 nM. At 24 hpi, cells were washed 3x with PBS and fixed with 4% paraformaldehyde at room temperature for 15 min. Fixed cells were washed 3x in PBS. DAPI was diluted to 2 μ g/ml in PBS +2% FBS. Samples were incubated with DAPI for 5 min. Coverslips were washed 3x in PBS and mounted on slides with ProLong Diamond (Life Technologies). Coverslips were sealed with nail polish before ProLong set to preserve the depth of the samples. Samples were imaged on a Zeiss LSM 700 Confocal Laser Scanning Microscope using a 63X/1.4 Plan Apo Oil objective lens and Zeiss ZEN 2011 software. ImageJ⁶³ and the plugin DeconvolutionLab2⁶⁴ were used to deconvolve the images. Two technical replicates, each with three biological replicates were made. The images used in the analysis consisted of 4 images of WT containing 23 macrophages and 295 bacteria.

Glucose uptake assay

Untreated or MCC950-treated BMDMs were infected at MOI 10 for 1 h with *S. aureus* LAC as above. After 1 h, 50 μ g/ml gentamicin was added, and cells were incubated for 24 h. At 24 h, glucose uptake was measured by Glucose Uptake-Glo Assay Kit (Promega) per manufacturer's instructions. Experiments were performed in biological triplicate twice on two separate days (n = 6). Statistical significance was determined using a one-way ANOVA with Sidak's multiple comparison.

Seahorse XF Glycolysis Stress Assay

BMDM were seeded at 8×10^4 cells/well in a 96 well Seahorse XF culture microplate (Agilent). BMDM were allowed to adhere overnight at 37°C with 5% CO₂ in complete MEM as described above. BMDMs were primed for 4 h with 10 ng/ml LPS. Wells were washed one time Seahorse DMEM (Agilent) and treated with 100 μ M MCC950 or vehicle control for 10 min α -toxin (Sigma) was added to the indicated wells at a final concentration of 50 ng/ml in 180 μ L. Samples were put on the Seahorse XF analyzer within 20 min of α -toxin addition. Seahorse XF Glycolysis Stress Test Kit was used following the manufacturer's instructions. The Seahorse XF Stress Test Report Generator was used to analyze and summarize the data. For each condition, 12 wells of BMDM were treated with inhibitor and/or toxin (n = 12). Statistical significance was determined using one-way ANOVA with Sidak's multiple comparison.

Relative ATP measurement

S. aureus strain LACluxABDCE was used to infect BMDMs at MOI 10 as above. At indicated timepoints, BMDMs were washed and lysed as described above. Luminescence was read on Biotek Synergy H1 microplate reader. RLU were normalized to CFU. Data shown are representative of 2 independent assays of 3 biological replicates (n = 6). Statistical significance was calculated using unpaired t-test (two-tailed).

Murine bacteremia model

For mouse infections, 8–10-week-old female mice were infected with $\sim 5 \times 10^6$ CFU of *S. aureus* strain HG003 or HG003 Δhla in 100 μ L PBS by intravenous (iv) injection. 1 h prior to infection, mice were administered 50 mg/kg MCC950 sodium in PBS (Selleck Chem #CP-456773) or vehicle control (PBS) by intraperitoneal (ip) injection. Rifampicin (Fisher Biochemicals) was dissolved in vehicle (6.25% DMSO +12.5% PEG300) at a final concentration of 6.25 mg/ml. At 24hpi, mice were treated with 25 mg/kg rifampicin or vehicle control by ip injection. At 48hpi, mice were euthanized via CO₂ asphyxiation followed by cervical dislocation. Spleens and livers were harvested, homogenized, serially diluted, and plated on TSA plates for enumeration of bacterial CFU. Percent rifampicin tolerant cells was determined by comparing survivors after rifampicin treatment to survivors of the vehicle treated group. Wild type mice: WT LAC vehicle n = 14 and WT LAC rifampicin n = 14, HG003 Δhla vehicle n = 5, HG003 Δhla rifampicin n = 5. The median is indicated by a horizontal line. Statistical significance was calculated using the Kruskal Wallis One-Way ANOVA with Dunn's multiple comparison or the Mann-Whitney test as described in the Figure legends. Blinding or randomization was not necessary as all outputs (CFU/g tissue) are objective.



QUANTIFICATION AND STATISTICAL ANALYSIS

Statistical analysis was performed using Prism 9 (GraphPad) software. For the *in vivo* studies, *n* represents the number of mice per group and statistical significance was determined using the Kruskal–Wallis one-way ANOVA with Dunn’s multiple comparison test or the Mann–Whitney test. For the *in vitro* studies, *n* represents the number of biological replicates and statistical significance was determined using a one-way ANOVA with Sidak’s multiple comparison test or an unpaired two-tailed *t*-test, as indicated in the Figure legends. The statistical methods and sample sizes (*n*) are indicated in methods for each experiment. Statistical significance was defined as $p < 0.05$. For CFU graphs of animal experiments the median is shown as a horizontal line. In all other Figures error bars show standard deviation.